

Study the Recycling of Red Mud in Iron Ore Sintering Process

Ahmed Abdelazim Khalifa^{1*}, Vladimir Yurievich Bazhin², Kuskova Yana Vadimovna³, Ahmed Abdelrahim⁴, Yasser Momtaz Zaki Ahmed⁵

¹ Department of Metallurgy, Saint Petersburg Mining University, St. Petersburg, 2, 21st Line, St Petersburg 199106, Russia

² Department of Minerals Technology and Processing, Central Metallurgical Research and Development Institute (CMRDI), P.O. Box 87, Helwan, Cairo, Egypt

³ Department of ATP, St. Petersburg mining University, St. Petersburg, 2, 21st Line, St Petersburg 199106, Russia

⁴ Process Metallurgy Research Group, Faculty of Technology, University of Oulu, Finland

⁵ Refractory and Ceramic Materials Department, Advanced Materials Division, Central Metallurgical Research and Development Institute, CMRDI, PO. Box 87, Helwan, Cairo, Egypt

* Corresponding author's e-mail: engahmedkhalifa2@gmail.com

ABSTRACT

Red mud (RM), the by-product generated during the alumina extraction process, is considered a valuable secondary raw material, since iron (20–54%) represents its major constituent. Accordingly, the suitability of recycling this RM in the sintering process of Egyptian iron ore was studied. The effect of adding different amounts of RM to the sinter charge mixture (0–10 wt.%) on the sintering process performance as well as the chemical, physical and mechanical properties of the produced sinter was investigated. The results revealed that increasing the amount of red mud in the sinter charge mixture leads to a high improvement in the strength of the produced sinter till reaching a maximum at 7% addition, which deteriorates thereafter. Meanwhile, owing to the fine nature of the red mud, increasing its contents in the sinter charge mixture leads to reduced speed of the sintering process, which consequently affects the productivity at the blast furnace yard. The sinter produced with the addition of 3% red mud shows the highest reducibility. These results indicate the suitability of recycling RM in the Egyptian iron ore sintering process with an amount not higher than 3 wt.% of the total sinter mixture charge.

Keywords: red mud, utilization, Egyptian iron ore, sintering process, sinter charge mixture, sinter strength and sinter production.

INTRODUCTION

Red mud (RM) is the tailing produced during the extraction of alumina from bauxite ore using the Bayer's process. In this process, bauxite ore is digested with sodium hydroxide to produce alumina which leads to the formation of huge amounts of tailing assigned as red mud [11–24]. In total global red mud production in 2019 was approximately 4 billion tones [21, 31, 34]. At present, about 0.15 billion tons of red mud are discharged annually to the environment either into the sea or artificial ponds/lakes, all over the world [15].

Approximately 8 tons (RM) are produced each year in Russia, of which more than 2 million from the Ural aluminum plant and about 600 million tons of RM are already accumulated in aluminum plants [22]. Almost all amounts of red mud are currently deposited in space-occupying and polluting landfill sites [23]. Therefore, due to the huge volumes produced and the negative effects of its disposal such as the ecological and environmental problems of land and polluting underground water, swamping, expensive management costs of red mud storage, red mud management is a global concern facing the alumina industries [13].

The collapse of a red mud reservoir in 2010 in western Hungary, resulted in the release of approximately one million cubic meters of red mud (with a pH of approximately 12), resulting in the deaths of ten people, while 150 were infected by various diseases [34]. The red mud produced from the treatment of various bauxite ore usually contains a high percentage of iron, aluminum, and titanium in oxide forms with the presence of some rare earth elements like scandium and vanadium [28]. Thus, the comprehensive utilization of this red mud via its recycling in different applications has received a lot of attention [10, 14, 17].

During the last few decades, many technologies for the utilization of red mud have been proposed such as building materials [5, 19] pigments, catalysts [12], adsorbent, and the recovery of valuable metals such as iron, titanium dioxide, scandium and alumina [2]. However, the application of red mud in these fields is restricted by volume, efficiency, costs, and the risks associated with mud [18, 33]. According to the fact that iron oxide represents the major constituents of this red mud, its utilization in the steel industry was regarded as the most intense and interesting application [1, 4, 25].

Recycling and utilization of iron-bearing residues have long been promoted in the sinter production for blast furnace iron making due to various reasons, including: the changes in the quality of world iron ore reserves due to the heavy demand; Reduction of dust emissions by improvement of sinter quality; Strict environmental legislation and to save energy [7].

The utilization of red mud as additive to the sinter charge mixture for iron ore sinter production has been previously studied in several works. Utkov et al. [30] indicated that adding up to 2% red mud in sinter mix improved the sinter strength, reduced the dust content, increased productivity, and reduced coke consumption in blast furnace operation. Moreover, using RM instead of bentonite in the sintering of iron ore contributes to a 5% increase in the productivity of sintering machines. Podgorodetskiy et al. [20] claimed that increasing low alkaline red mud in the sintering of iron ore promoted the formation of the crystal ferritic phase which leads to an increase in the sinter strength and decrease of agglomerate attrition. In Greece, the technology of multiple red mud recycling to obtain pig iron and mineral wool for use in the construction industry was studied on a pilot-plant scale [3].

Some investigations on the use of red mud in an iron ore sintering plant revealed that the addition of blue dust with red mud to the iron ore sinter mixture charge would overcome the problems arising from the RM addition to the sinter charge, like dilution of the sinter iron content, sinter quality, strength and productivity [26]. Trushko et al. [28] found that replacement of the initial iron ore concentrate with 2 wt.% red mud increased the overall sinter strength, as well as the productivity. It was also found that by increasing the Al_2O_3 content in the blast furnace batch, the transfer of the alkali present to the slag phase is facilitated. Easier transfer of alkalis to the slag reduces the viscosity of the slag and reduces the sulfur content of the hot metal. On the other hand, the effect of RM addition on the types of phases formed in the produced sinter was investigated [27]. It was reported that the amorphous silicate binders in the sinter are replaced by ferrite crystals with increased percentage of RM, which consequently enhances the produced sinter strength.

However, the main drawback of the RM is its high alkalinity, which is regarded as the primary reason for its lack of industrial application. This drawback is not found in the RM utilized in this investigation, according to the fact that the JSC Ural Aluminum Plant has introduced the current production of red mud by lime milk treatment in the flow channel-like reactor named dealkalization technology [26].

On the other hand, the main gangue minerals associated with the Egyptian iron ore deposits used for the sintering process in the Egyptian Iron and Steel Co. include barium oxide, manganese oxides, and alumina. The presence of these oxides in the produced iron ore sinter as blast furnace charge leads to disturbing the blast furnace operation with high fuel consumption during pig iron production. Accordingly, the Egyptian researchers working in the iron and steel field have developed a suitable mineral processing technology to treat this ore and eliminate most of these gangue minerals. The produced iron ore concentrate was found to have the iron content that reaches about 74% Fe_2O_3 with acceptable contents of impurities. The concentrate with this chemical composition is a good candidate to produce sinter with reasonable quality with small variation in chemical analysis in order to operate a blast furnace at a steady state rate with low fuel consumption. It was earlier reported that [16], in order to achieve a steady state blast furnace operation, The blast furnace charge

(the iron ore sinter) should contain high iron content with limited Na_2O content (below 0.5%), Al_2O_3 content (below 5%), TiO_2 content (below 3%) with minimum harmful impurities like S, P, and Zn. In addition, it should have an acceptable ratio of silica, calcia, and alumina for facilitating the blast furnace operation. In this investigation, in order to fulfill these requirements, the maximum RM addition to the iron ore concentrate sinter charge was determined to be 10%.

The aim of this research is the partial replacement of the Egyptian iron ore concentrate in the sintering operation by low alkaline red mud and studying the effect of different amounts of red mud addition on the quality, reducibility, phase composition, and microstructure of the produced sinter.

EXPERIMENTAL WORK

Materials and Procedure

El-Baharia iron ore, limestone, recycled sinter (sinter return), coke breeze, and low alkaline red mud are the raw materials used for this

work. These raw materials were collected from an Egyptian iron and steel company Helwan, Cairo, Egypt. El-Baharia iron ore was subjected to mineral processing operation for producing an iron ore concentrate at Central Metallurgical Research and Development Institute, (CMRDI), Cairo, Egypt. The low alkali- red mud samples were obtained from Ural aluminum plant, (Ural, Russia).

The total chemical composition of RM, iron ore concentrate, coke breeze, and ash analysis were obtained using X-ray fluorescence spectroscopy (XRF) and presented in tables 1 and 2. The size distribution of iron ore concentrates, limestone, and red mud are shown in table 3. The range of particle size for iron ore varies from 0.105 mm to 10 mm, whereas in RM, particles are present in 0.105mm to 2 mm size ranges.

The phase composition of the RM was determined by X-ray diffraction (XRD), Bruker Axs D8 Advance, Germany) with $\text{Cu } \alpha$ radiation. Figure 1, illustrates the main phase composition of RM which are hematite (Fe_2O_3), kaolinite ($\text{Al}_2\text{Si}_2\text{O}_5(\text{OH})_4$), calcite (CaCO_3), and quartz (SiO_2).

Firstly, all materials were dried at 110°C for 2 hrs, before the preparation of iron ore mixture

Table 1. Composition of the raw material used for sintering

Compositions. %	Iron concentrate	Limestone	Sinter return	Red mud
Fe total	52.16	-	53.74	35.01
Fe_2O_3	74.51	-	61.05	50.02
FeO	-	-	14.15	-
SiO_2	9.14	1.05	8.76	7.14
Al_2O_3	2.06	0.78	2.20	12.73
CaO	1.90	54.69	8.17	15.00
MgO	0.35	0.12	0.96	1.01
P_2O_5	0.44	0.07	0.52	0.93
MnO	3.15	-	2.46	0.21
Na_2O	0.34	0.18	0.19	0.85
K_2O	0.40	0.070	0.08	0.11
Cl	0.40	0.1	-	-
TiO_2	0.16	-	0.05	5.70
BaO	1.3	-	1.17	-
ZnO	0.08	-	0.14	-
S	0.65	0.04	0.10	0.90
CO_2	-	42.90	-	-
L.O.I*	5.12	-	-	5.40

* Is the loss of ignition

Table 2. The proximate analysis of coke breeze and chemical compositions of ash

Item	Fixed C. (%)	Volatiles (VM) (%)	Ash (%)	Sulphur (%)	Ash (%)			
					CaO	SiO_2	Al_2O_3	Others
Coke breeze	88.66	1.08	10.26	1.18	0.70	3.00	2.00	4.56

Table 3. Size distribution of iron ore concentrates, limestone and coke breeze

Size, mm	Iron ore fines, %	Limestone %	Coke breeze, %	RM, %
-10+8	5.6	-	-	-
+6.35	8.2	-	-	-
+4.0	15.9	-	-	-
+3	7,5	2.27	-	-
+2	6.96	15.72	20.80	2.4
+1	11.3	18.27	26.59	11.6
+0.59	10.35	13.65	15.45	35.7
+0.25	11.53	11.59	13.66	29.6
+0.17	7.86	12.19	9.65	11.4
+0.105	9.79	16.45	5.98	8.1
-0.105	4.61	9.86	7.87	1.2

charge. The sinter charge is composed of iron ore concentrate, limestone, coke breeze, and sinter return without and with different amount of RM. The sinter return is an iron ore sinter of particle size ranging from -7 mm and initially prepared (without RM addition) with the same operation. The importance of sinter return addition is to facilitate and improve the sintering operation. It represents 30% of the total weight of the mixture charge and fixed for all experiments. The coke breeze utilized had a size ranging from 1–3 mm. This coke breeze size was reported to be the best size for obtaining high-performance sintering operation [9]. The basicity of the sinter charge (CaO/SiO_2) was adjusted at 0.9 via controlling the amount of limestone addition and has been held constant for all experiments. The sinter charge mixture is granulated with the addition of an appropriate amount of water to provide a good sinter charge permeability during sintering operation. The granulated charge was then

charged to a laboratory sinter pot for performing the sintering experiments. The laboratory sinter pot has a raw sinter capacity of 5.0 kg, a bed diameter of 125 mm, and a height of 340 mm. The green charge (+10 mm) was mounted over the sinter bed layer. The green raw mixture was ignited with a natural gas flame at around 1150°C for 2 min. The ignition occurred at a suction pressure of 5.88 kPa, while the sintering process was conducted at a suction pressure of 11.76 kPa. Sintering time is the time from the ignition beginning till the maximum temperature of the exhaust gas was reached. After the experiment is finished, the cooling cycle continues until the temperature reaches under 100°C. In order to evaluate the effect of RM addition on the sintering process and the produced sinter quality, a charge without RM addition is firstly sintered and assigned as a reference sample (REF), then four sintering experiments with sinter mix charge of 3, 5, 7 and 10% RM content are carried out.

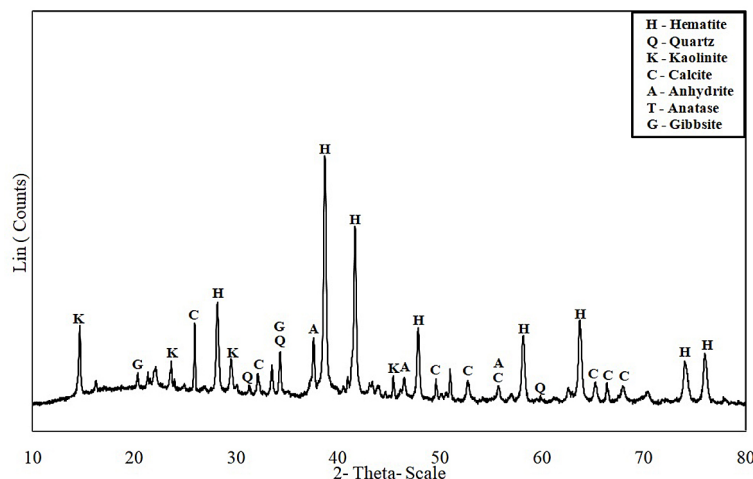


Figure 1. X-ray diffraction of red mud

Characterizations

Sinter strength is one of the essential requirements in the sintering process to prevent the disintegration of the sinter material and to improve the permeability in the blast furnace [6]. After sintering, the sinter strength is determined by using the shatter test. In the shatter test, the sinter cake was screened over a sieve of +7 mm, sinter of +7 mm was dropped four times from a height of 2 m, then the output of sinter after the shatter tester was screened again over a sieve of 7 mm. The sinter strength (S_s) was calculated as the percentage of (+7 mm) sinter after the shatter test relative to +7mm before the shatter test using the following equation.

$$\text{Sinter Strength } (S_s) \% = \left[\frac{W_3}{W_1} \right] \times 100 \quad (1)$$

where: W_1 is the weight of sinter of +7 mm before shatter test, kg.

W_3 = weight of sinter of +7mm after shatter test, kg.,

The production of the sintering machine (P), and the sinter machine at blast furnace yard (PB.F) were calculated according to the following equations, as described before [7].

$$(P) \% = 14.4. K. \rho V \times 100 \text{ ton/m}^2.\text{day} \quad (2)$$

where: K is the percentage (above 7mm) of ready-made sinter of the charge,

$$\text{Ready made sinter } (K) \% = \left[\frac{W_1}{W_1 + W_2} \right] \times 100 \quad (3)$$

where: W_1 is the weight of sinter of +7 mm and W_2 = weight of sinter of -7mm before shatter test, kg.

ρ is bulk density of the charge, ton/m³,
 V is vertical velocity of sintering machine

$V = \frac{H}{T}$ m/min . H is the height of the charge in the sinter pot.

T is the time of sintering, min.,

$$(P_{B.F}) \% = P \times S_s \text{ ton/m}^2 \text{ per day} \quad (4)$$

where: $P_{B.F}$ is the productivity of the sinter machine at blast furnace yard, expressed in ton/m² per day,

P is the productivity of sintering machine, also expressed in ton/m² per day and

S_s % is the sinter strength above 7 mm.

The produced sinters were subjected to the microstructure examination using a light microscope. The sinter grains of ~1 to 3 mm size were mounted in Bakelite, ground and polished using 1 μ m alumina (Al_2O_3) solution. The specimens of sinters with different red mud contents were examined.

The reduction behavior of the produced sinters was investigated using hydrogen gas at 1.5 l/ min flow rate using a thermo-gravimetric apparatus, which is described elsewhere [8]. The samples were firstly dried at 110°C for 2 hrs to remove moisture, and then they were transferred to the furnace. The furnace was heated to the desired temperature (800 °C) and kept constant to $\pm 5^\circ C$. Nitrogen gas was passed through the thermo-gravimetric furnace at the beginning and at the end of the reduction to flush air out for each experiment. During the reduction process, the sinter sample weight was continuously determined using a scale connected to a computer system. The reducibility degree was calculated using the following equation:

$$\begin{aligned} \text{Percentofreduction}(R) &= \\ &= \left[\frac{(W_0 - W_t)}{\text{Oxygenmass}} \right] \times 100 \end{aligned} \quad (5)$$

where: W_0 : the initial mass of the sample after moisture removal.

W_t : the mass of the sample after each time, t.

Oxygen (mass): the mass of oxygen percentage in the sample in the form of FeO & Fe₂O₃.

RESULTS AND DISCUSSION

Effect of added red mud on sinter strength

Figure 2 illustrates the variation of both sinter strength and ready-made sinter with changing the content of RM in the sinter charge mixture. It was found that increasing the RM content leads to an increase in both sinter strength and ready-made

sinter till reaching a maximum at 7% RM content, which decreases thereafter. The increase in the sinter strength and consequently the amount of the ready-made sinter could be attributed to the fact that the RM addition is responsible for rising the hot zone temperature during the sintering process which enables the creation of more melting points in the sinter charge. On the other hand, it was previously confirmed that adding low alkali bauxite residue to sinter blends leads to the formation of much more amounts of Al-Si ferrites in the high-temperature sintering zone with a decrease in the amount of glass phase formation. Meanwhile, increasing the RM content (which has a small particle size) beyond 7% leads to a disturbance in the sinter bed thermal efficiency due to the deterioration in the bed permeability occurring as a result of increasing fineness in the sinter charge blend [9]. In addition, the presence of alumina in the form of kaolinite in the added RM plays an important role in improving the sinter strength. Alumina promotes the formation of the SFCA phase, which has a positive effect on the sinter strength. However, the sharp increase in the RM content would lead to the formation of a large amount of glassy phases, which is the main cause concerned for the lower sinter strength.

Effect of red mud on vertical velocity and sintering productivity

Figure 3 shows the effect of the sinter charge RM content on the vertical velocity of the sintering process. It can be observed that the vertical velocity of sintering has progressively decreased with red mud addition. Thus, it was noted that the

high fineness of red mud wastes would contribute to decrease the granulation efficiency and reduces the vertical velocity. Granulation efficiency has an influence on bed permeability, airflow rate in the sinter bed, the rate of descent of the flame front, and the bed temperature profile as a function of time [29].

The effect of the sinter charge RM content on both the productivity of the sintering machine and the productivity at the blast furnace yard is shown in Figure 4. It was found that increasing of the RM content leads to a slight decrease in both the productivity of the sintering machine and the blast furnace yard appeared to drop obviously. The decrease in both productivities could be explained by the high fineness of RM, which might decrease the permeability of the sintering charge, subsequently decreased the vertical velocity of the sintering process, as mentioned before. This directly causes a decrease in the sinter production. Therefore, the optimal content of red mud should be controlled within 3–5%

XRD analysis

Figure 5 shows the XRD patterns of sinter produced from the charges containing different RM contents. The XRD patterns revealed that REF produced a sinter sample (sample without RM addition) composed of hematite (H), magnetite (M), wustite (W), SFCA (S), and calcium silicate (C). With increasing the RM content, a slight decrease of the hematite phase with a corresponding increase in the magnetite phase is clearly noticeable. In addition, it can be easily noticed that increasing the RM content leads to an increase in

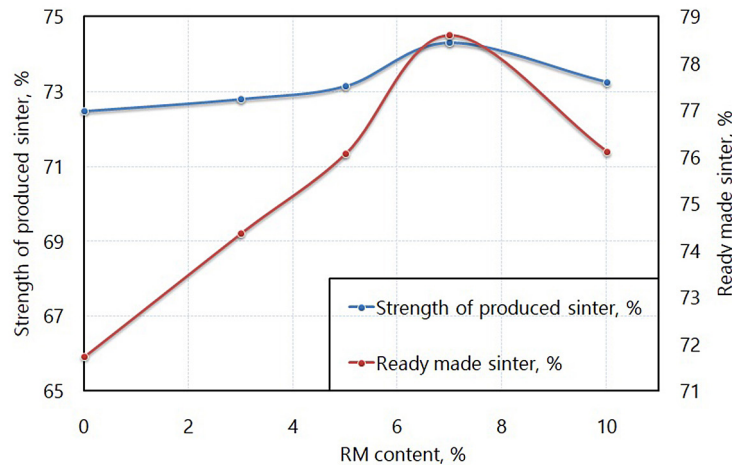


Figure 2. Effect of RM content on sinter strength and ready-made sinter

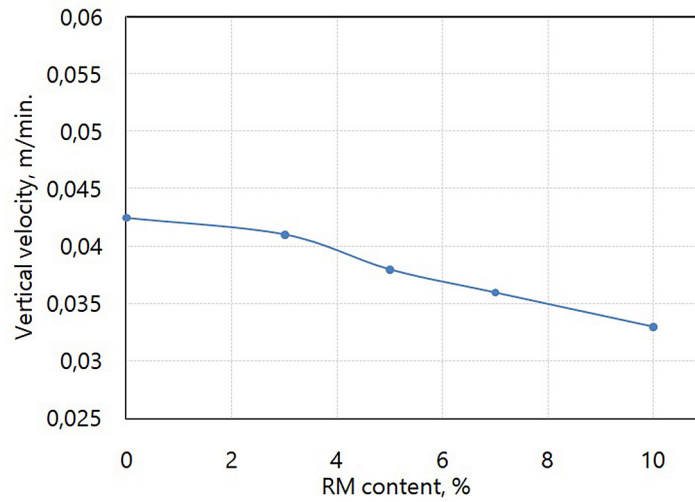


Figure 3. Effect of RM content on the vertical velocity of sintering process

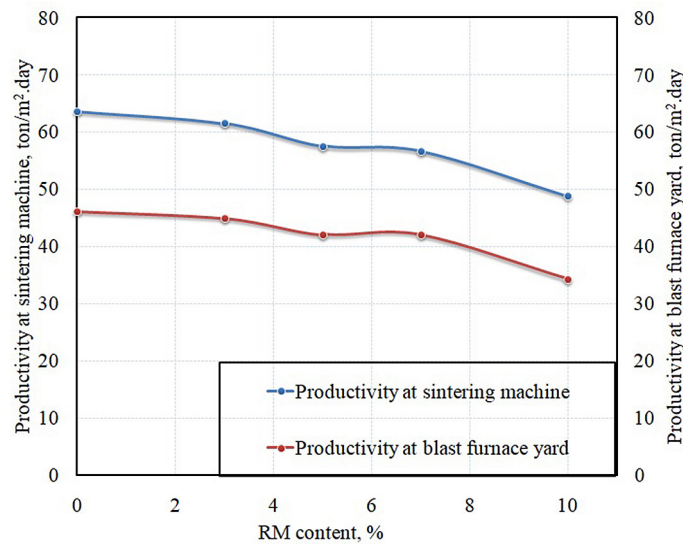


Figure 4. Effect of RM content on the productivity of sintering machine and B.F yard

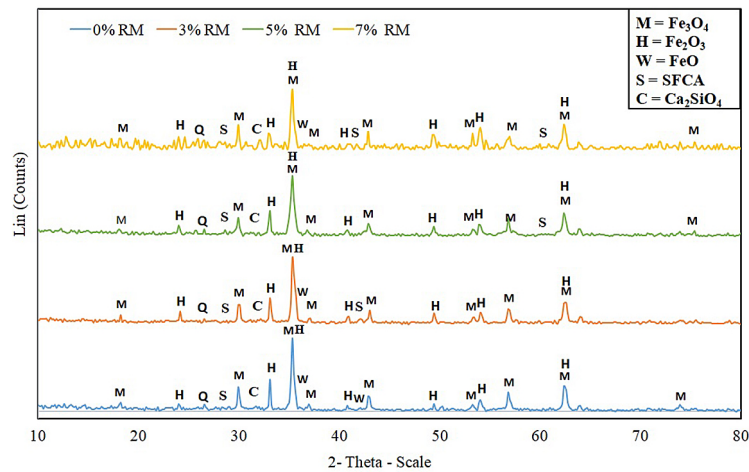


Figure 5. X-ray diffraction of the produced sinter with different RM content

β - Ca_2SiO_4 phase formation. The formation of this phase without its transformation to γ - Ca_2SiO_4 is related to the presence of TiO_2 in the added RM. It was earlier reported that TiO_2 would act as a stabilizer to the β - Ca_2SiO_4 phase preventing its transformation into γ - Ca_2SiO_4 phase. The formation of the γ - Ca_2SiO_4 phase is responsible for increasing the volume by about 10% and this expansion responsible for the deterioration in the final sinter strength. This stabilization could be another reason for the increase of the sinter strength with increasing RM content.

Effect of RM content on Sinter Microstructure

The microstructure at different areas in the sinter samples has been thoroughly examined to be able to determine the effect of the RM content on the microstructure of the produced sinter. Figure 6 shows the microstructure of the sinter samples produced from charge without and with different RM contents. The general observation revealed that the addition of RM fundamentally changes the microstructure of the produced

sinters (Fig. 6A-E). The microscopic examinations of REF sinter sample (Fig. 6A) indicate that it is mainly composed of magnetite (white), hematite (grey), silicate phases with little SFCA, and (black) pores. Increasing the RM content leads to a decrease in the hematite and increasing the silicate and SFCA phases. The increase in the silicate forming component (Al-Si ferrite) and decrease amount of glass phases, with increasing RM content is in agreement with observations by Podgorodetskiy et al. [20]. As a result, the strengthening of the properties of sintering materials has been improved. In the case of the sinter containing 5% RM (Fig. 6C), the hematite on the surface is characterized by large numbers of small pores. In the sinter containing 7% RM hematite, magnetite, calcium ferrite, dicalcium silicate and slag were detected. The amount of calcium ferrite phase was increased along with the RM content to 7%, as shown in Fig. 6D). The β - Ca_2SiO_4 formation was one of the significant microstructural features found when adding RM. The presence of oxides minerals that existed in RM (such as Al_2O_3 , SiO_2 , TiO_2 , and

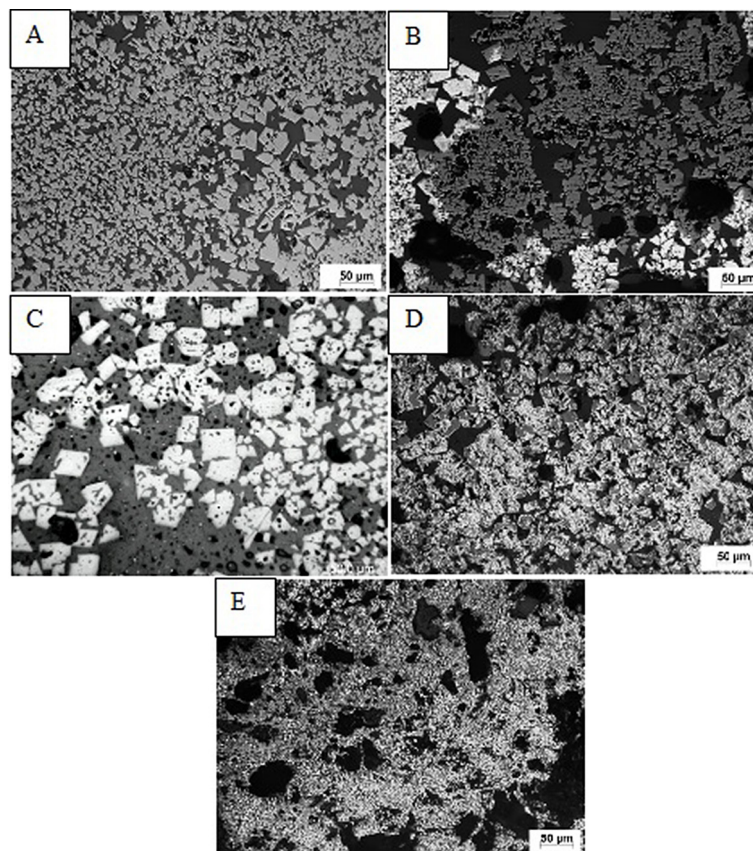


Figure 6. Microstructure of sinter containing 0–10% red mud, (A) 0% RM, (B) 3% RM, (C) 5% RM, (D) 7% RM and (E) 10% RM. (black = pore, white and gray = magnetite and hematite, and dark gray = glass phase and some larnite (β - Ca_2SiO_4))

P_2O_5) may have contributed to stabilizing the $\beta-Ca_2SiO_4$ up to room temperature. Moreover, the presence of silicate in the sinter melt could have a similar effect and enhance the formation of $\beta-Ca_2SiO_4$ [6].

Reduction of produced sinter

Figure 7 illustrates the reducibility of sinter produced without and with different RM contents. It was found that the sinter containing 3% RM shows the highest reducibility with a reduction degree reaching about 86%. Increasing the RM content beyond 3% leads to a tremendous deterioration in the sinter reducibility. This behavior could be attributed to the role of alumina in the produced sinter. With the first addition of RM (at 3%) the amount of alumina is consumed in the formation of SFCA phase, this phase is responsible for improving the gas permeability and

consequently the sinter reducibility [32]. On the other hand, a large increase in the RM content (beyond 3%) is responsible for increasing the melt formation during the sintering process leads to the formation of more slag phases and dense microstructure (as shown in Fig 6) and consequently retards the sinter reducibility. This result indicates that the addition of 3% RM to the sinter charge produced the sinter with the highest reducibility, acceptable sinter properties, and reasonable sintering operation parameters. Accordingly, 3% RM addition is regarded as the most suitable addition for producing the iron ore sinter from the Egyptian iron ore concentrate.

The XRD pattern of sinter produced with 3% RM content after reduction is shown in Figure 8. The pattern revealed that the major phase of the reduced sinter is metallic iron with the presence of minor phases of both magnetite and calcium silicate.

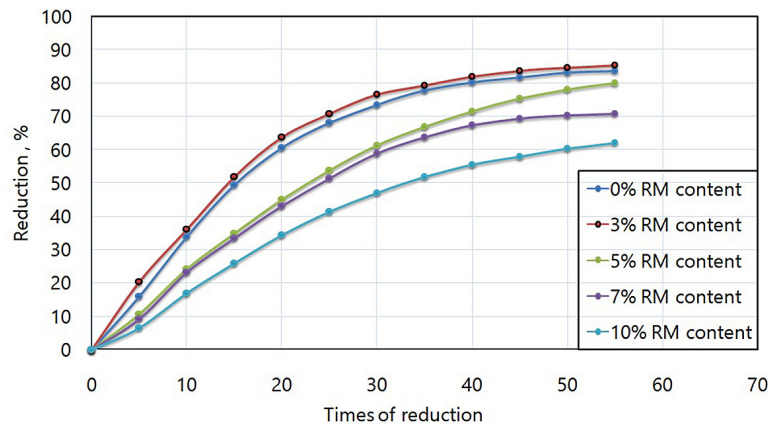


Figure 7. Effect of RM content on the sinter reducibility

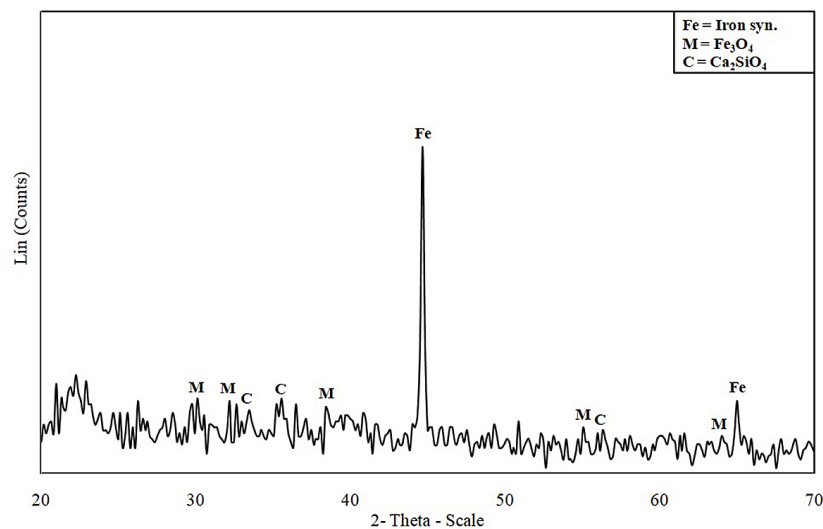


Figure 8. X-ray diffraction of the 3 % RM produced sinter reduced at 800 °C

CONCLUSIONS

The effect of red mud on the sintering behavior was researched. The following conclusions were drawn:

1. Both sinter strength and ready-made sinter first increase along with the RM content until reaching a maximum at 7% RM content, decreasing thereafter. The productivity of both the sinter machine and blast furnace yard appeared to drop obviously with the increasing RM content. The principal effect on productivity is vertical velocity sintering which also significantly decreased due to its fine particle size of red mud, which decreased the permeability of the sinter bed, by adding more RM.
2. The reducibility of produced sinter is slightly increased at 3% RM, reaching about 86%. The improvement of the reduction with 3% RM addition could attribute to the effect of the Al_2O_3 content in the produced sinter, which consumed in the formation of SFCA and consequently enhanced the reducibility of the sinter.
3. The $\beta-Ca_2SiO_4$ formation was one of the significant microstructural features found when adding RM.
4. The main phases of reduced sinter with 3% RM are metallic iron, magnetite, and dicalcium silicate.

Acknowledgments

The authors wish to express thanks to the Egyptian Ministry of Higher Education and Scientific Research for funding the scholarship of the corresponding author.

REFERENCES

1. Agrawal S., Rayapudi V., and Dhawan N. 2018. Microwave Reduction of Red Mud for Recovery of Iron Values. *Journal of Sustainable Metallurgy*, 3(4), 427–43. doi: 10.1007/s40831-018-0183-3.
2. Alkan G.C. Schier, Gronen L., Stopic S., and Friedrich B. 2017. A Mineralogical Assessment on Residues after Acidic Leaching of Bauxite Residue (Red Mud) for Titanium Recovery. *Metals*, 7(11), 1–11. doi: 10.3390/met7110458.
3. Balomninos E. Kastritis D., Panias D., Paspaliaris I., and Boufounos D. 2014. The Enxal Bauxite Residue Treatment Process: Industrial Scale Pilot Plant Results. *Light Metals 2014*, 141–47. doi: 10.1002/9781118888438.ch25.
4. Bhoi, B., Rajput P., and Mishra C.R. 2012. Processing of Red Mud by Low Temperature Microwave Hydrogen Plasma for Production of Iron : An Eco-Friendly Technology. *Processing of Red Mud by Low Temperature Microwave Hydrogen Plasma for Production of Iron: An Eco-Friendly Technology*, 19, 79–684.
5. Deelwal K., Dharavath K., and Kulshreshtha M. 2014. Evaluation of Characteristic Properties of Red Mud for Possible Use as a Geotechnical Material in Civil Construction. *International Journal of Advances in Engineering & Technology*, 7(3), 1053–59.
6. Dehghan-Manshadi A., Manuel J., Hapugoda S., and Ware N. 2014. Sintering Characteristics of Titanium Containing Iron Ores. *ISIJ International*, 54(10), 2189–95. doi: 10.2355/isijinternational.54.2189.
7. El-Hussiny N.A., Mohamed F.M., and Shalabi M.E.H. 2011. Recycling of Mill Scale in Sintering Process. *Science of Sintering*, 43(1), 21–31. doi: 10.2298/SOS1101021E.
8. El-Hussiny N.A., Khalifa A.A. El-midany A.A. Ahmed A.A. and Shalabi M.E.H. 2015. Effect of Replacement Coke Breeze by Charcoal on Technical Operation of Iron Ore Sintering. *International Journal of Scientific & Engineering Research*, 6(2), 681–686
9. Fouzi S.M., Kahlifa M.G., Ahmed Y.M.Z., Mohamed F.M., and Shalabi M.E.H. 2006. Sintering of Egyptian Iron Ore.” *Górnictwo i Geoinżynieria*, 30(3/1), 91–107.
10. Khalifa A.A., Utkov V.A., and Brichkin V.N. 2020. Red Mud Effect on Dicalcium Silicate Polymorphism and Sinter Self-Destruction Prevention. *Proceedings of Irkutsk State Technical University*, 24(1), 231–40. doi: 10.21285/1814-3520-2020-1-231-240.
11. Lebedev A.B., Utkov V.A., and Bazhin V.Yu. 2019. Use of Red Mud as a Modifier in Granulation of Metallurgical Slags. *Proceedings of Irkutsk State Technical University*, 23(1), 158–68. doi: 10.21285/1814-3520-2019-1-158-168. (In Russian).
12. Liu Q., Xin C. Li C., Xu C., and Yang J. 2013. Application of Red Mud as a Basic Catalyst for Biodiesel Production. *Journal of Environmental Sciences*, 25(4), 823–29. doi: 10.1016/S1001-0742(12)60067-9.
13. Liu Y, and Naidu R. 2014. Hidden Values in Bauxite Residue (Red Mud): Recovery of Metals. *Waste Management*, 34(12), 1–12.
14. Luo M., Qi X., Zhang Y., Ren Y., Tong J., Chen Z., Hou Y., Yeerkebai N., Wang H., Feng S., and Li F. 2017. Study on Dealkalization and Settling Performance of Red Mud. *Environmental Science and Pollution Research*, 24(2), 1794–1802. doi: 10.1007/s11356-016-7928-y.

15. Lyu F., Gao J., Sun N., Liu R., Sun X., Cao X., Wang L., and Sun W. 2019. Utilisation of Propyl Gallate as a Novel Selective Collector for Diaspore Flotation. *Minerals Engineering*, 131, 66–72. doi: 10.1016/j.mineng.2018.11.002.
16. Mozhareno N., and Noskov V. 2005. Effect of Red Mud on the Metallurgical Properties of Sinter. *Fundamental and Applied Problems of Ferrous Metallurgy*, 10(10), 62–70.
17. Mukiza E., Zhang L.L., Liu X., and Zhang N. 2019. Utilization of Red Mud in Road Base and Subgrade Materials: A Review. *Resources, Conservation and Recycling* 141, 187–99. doi: 10.1016/j.resconrec.2018.10.031.
18. Pan X., Yu H., and Tu G. 2015. Reduction of Alkalinity in Bauxite Residue during Bayer Digestion in High-Ferrite Diasporic Bauxite. *Hydrometallurgy*, 151, 98–106. doi: 10.1016/j.hydromet.2014.11.015.
19. Piirainen V., Yu, Boeva A.A., and Nikitina T.Y. 2020. Application of New Materials for Red Mud Immobilization. *Key Engineering Materials*, 854, 182–87. doi: 10.4028/www.scientific.net/KEM.854.182.
20. Podgorodetskiy G., Gorbunov V., Panov A., Petrov S., and Gorbachev S. 2015. Complex Additives on the Basis of Red Mud for Intensification of Iron-Ore Sintering and Pelletizing, 107–11. doi: 10.1002/9781119093435.ch20.
21. Pontikes Y., and Angelopoulos G.N. 2013. Bauxite Residue in Cement and Cementitious Applications: Current Status and a Possible Way Forward. *Resources, Conservation and Recycling*, 73, 53–63. doi: 10.1016/j.resconrec.2013.01.005.
22. Pyagay I.N. 2016. The Block Processing of Red Mud of Alumina Production. *Tsvetnye Metally*, 7, 43–51. doi: 10.17580/tsm.2016.07.05.
23. Pyagay I.N., Kozhevnikov V.L., Pasechnik L.A., and Skachkov V.M. 2016. Processing of Alumina Production Red Mud with Recovery of Scandium Concentrate. *Journal of Mining Institute*, 218, 225–32.
24. Sai P.S., Pradesh A., Sukesh C., and Pradesh A. 2017. Strength Properties of Concrete by Using Red Mud as a Replacement of Cement with Hydrated Lime. *International Journal of Civil Engineering and Technology (IJCIET)*, 8(3), 38–49.
25. Samouhos M., Taxiarchou M., Tsakiridis P.E., and Potiriadis K. 2013. Greek ‘Red Mud’ Residue: A Study of Microwave Reductive Roasting Followed by Magnetic Separation for a Metallic Iron Recovery Process. *Journal of Hazardous Materials*, 254–255(1), 193–205. doi: 10.1016/j.jhazmat.2013.03.059.
26. Shiryayeva E.V., Podgorodetskiy G.S., Malysheva T.Y., Gorbunov V.B., Zavodyanyi A.V., and Shapovalov A.N. 2014. Effects of Adding Low-Alkali Red Mud to the Sintering Batch at OAO Ural’skaya Stal’. *Izvestiya VUZ. Chernaya Metallurgiya*, 44(1), 6–10. doi: 10.3103/S0967091214010173.
27. Trushko V.L., and Utkov V.A. 2016. Development of Import Substituting Technologies for Increasing Productivity of Sintering Machines and Strength of Agglomerates. *Journal of Mining Institute*, 221, 675–80. doi: 10.18454/PMI.2016.5.675.
28. Trushko V.L., Utkov V.A., and Sivushov A.A. 2017. Reducing the Environmental Impact of Blast Furnaces by Means of Red Mud from Alumina Production. *Steel in Translation*, 47(8), 576–78. doi: 10.3103/S0967091217080149.
29. Umadevi T., Brahmacharyulu A., Roy A.K., Mahapatra P.C., Prabhu M., and Ranjan M. 2011. Influence of Iron Ore Fines Feed Size on Microstructure, Productivity and Quality of Iron Ore Sinter. *ISIJ International*, 51(6), 922–29.
30. Utkov V.A., and Leontiev L.I. 2005. Increasing the Strength of Agglomerates and Pellets with Bauxite Red Mud. *Stal’*, 9, 2–4.
31. Wang Li, Hu G., Lyu F., Yue T., Tang H., Han H., Yang Y., Liu R., and Sun W. 2019. Application of Red Mud in Wastewater Treatment. *Minerals*, 9(5), 281.
32. Webster Nathan A.S., Mark I. Pownceby, Ian C. Madsen, CSIRO Process Science, and Clayton South. 2013. In Situ X-Ray Diffraction Investigation of the Formation Mechanisms of Silico-Ferrite of Calcium and Aluminium-I-Type (SFCA-I-Type) Complex Calcium Ferrites, 53(8), 1334–40.
33. Zhu X Feng, Zhang T., Wang Ya., Lü G., and Zhang W. 2016. Recovery of Alkali and Alumina from Bayer Red Mud by the Calcification–Carbonation Method. *International Journal of Minerals, Metallurgy and Materials*, 23(3), 257–68. doi: 10.1007/s12613-016-1234-z.
34. Zinoveev D.V., Grudinskii P.I., Dyubanov V.G., Kovalenko L.V., and Leont’ev L.I. 2018. Global Recycling Experience of Red Mud – a Review. Part i: Pyrometallurgical Methods. *Izvestiya Ferrous Metallurgy*, 61(11), 843–58. doi: 10.17073/0368-0797-2018-11-843-858.